Available online at www.sciencedirect.com
SCIENCE DIRECT®

Journal of Organometallic Chemistry 664 (2002) 27–36

Journal of Organo metallic Chemistry

www.elsevier.com/locate/jorganchem

Reactivity of *cyclo*-$(PhX)_6$ (X = As, P) towards $[M_3L_2(CO)_{10}]$ (M = Ru, L = CO or NCMe; M = Fe, L = CO)

Rohini M. De Silva [a], Martin J. Mays [a,*], Gregory A. Solan [b,*]

[a] *Department of Chemistry, Lensfield Road, Cambridge CB2 1EW, UK*
[b] *Department of Chemistry, University of Leicester, University Road, Leicester LE1 7RH, UK*

Received 11 August 2002; accepted 3 September 2002

Abstract

Reaction of $[Ru_3(CO)_{10}(NCMe)_2]$ with *cyclo*-$(PhX)_6$ (X = As **1a**, P **1b**) in toluene at ambient temperature gives $[Ru_3\{\mu\text{-}cyclo\text{-}(PhX)_6\}(CO)_{10}]$ (X = As **2a**, P **2b**), in which the intact six-membered rings adopt chair conformations and bridge metal–metal edges via either two arsine (**2a**) or two phosphorus (**2b**) atoms in the 1,5 positions of the respective rings. Conversely, treatment of $[Ru_3(CO)_{12}]$ with *cyclo*-$(PhX)_6$ (X = As **1a**, P **1b**) in toluene at elevated temperature results in fragmentation of the six-membered rings to afford $[Ru_4(\mu_3\text{-AsPh})_2(CO)_{13}]$ (**3**) and $[Ru_6(\mu_4\text{-PPh})_3(\mu_3\text{-PPh})_2(CO)_{12}]$ (**4**), respectively. Fragmentation of the *cyclo*-hexaarsane ring in **1a** also occurs on reaction with $[Fe_3(CO)_{12}]$ in toluene at elevated temperature to furnish $[Fe_3(\mu_3\text{-AsPh})_2(CO)_9]$ (**5**) as the sole product. However, treatment of **1b** with $[Fe_3(CO)_{12}]$ gives $[Fe_3(\mu_3\text{-PPh}_2)_2(CO)_9]$ (**6**), the phosphorus analogue of **5**, along with $[Fe_2\{\mu\text{-}\eta^2\text{-}catena\text{-}(P_4Ph_4)\}(CO)_6]$ (**7**) and $[Fe_2\{\mu_4\text{-}(P_2Ph_2)\}(CO)_6]_2$ (**8**). In addition, the mixed phosphinidene–arsenidene complex $[Fe_3(\mu_3\text{-PPh})(\mu_3\text{-AsPh})(CO)_9]$ (**9**) can be obtained on treatment of **1** with a 1:1 mixture of **1a** and **1b**. Single crystal X-ray diffraction studies have been performed on **2a**, **3**, **4**$\cdot 2CH_2Cl_2$, and **8**.

Keywords: Cluster; Ruthenium; Iron; Arsenic; Phosphorus

1. Introduction

The application of *cyclo*-polyarsanes (CPAs) $[(RAs)_n$, R = hydrocarbyl, $n = 4–6]$ and *cyclo*-polyphosphanes (CPPs) $[(RP)_n$, $n = 3–6]$ as reagents for the preparation of transition metal cluster complexes has been the subject of intense research activity [1–3]. This can be attributed, in part, to the diversity of structural types that are accessible, often containing unparalled hybrid transition metal-main group architectures, in which the CPA or the CPP has ring-opened and fragmented to generate capping groups and chains (or combinations of both) based on RAs/RP units or unsubstituted Group 15 atoms.

As part of a programme investigating the chemistry of aryl-substituted hexameric members of the CPA and CPP families, we carried out an examination of their reactions with Group 9 transition metal carbonyl and mixed-metal Groups 8/9 carbonyl complexes under relatively mild conditions [4]. For example, cleavage and fragmentation of the *cyclo*-$(PhX)_6$ (X = As **1a**, P **1b**) ring is promoted by the room temperature addition of $[Co_2(CO)_8]$ [5–7], while the alkyne-bridged dicobalt complex $[Co_2(\mu\text{-CRCR})(CO)_6]$ and the thioxo-capped dicobalt–iron complex $[Co_2Fe(\mu_3\text{-S})(CO)_9]$ support the coordination of intact rings under similar conditions [8]. In the case of $[Co_2Fe(\mu_3\text{-S})\{\mu\text{-}cyclo\text{-}(PhP)_6\}(CO)_7]$, thermolysis leads to fragmentation of the coordinated *cyclo*-$(PhP)_6$ (**1a**) ring to give $[Co_2Fe(\mu_3\text{-SPPh})(\mu\text{-}\eta^2\text{:}\eta^2\text{:}\eta^1\text{-}P_5Ph_5)(CO)_5]$ as the sole reaction product.

Herein we are concerned with a study of the reactivity of **1a** and **1b** towards the homotrimetallic Group 8 transition metal carbonyl complexes $[Ru_3(CO)_{10}\text{-}(NCMe)_2]$, $[Ru_3(CO)_{12}]$ and $[Fe_3(CO)_{12}]$.

* Corresponding authors. Fax: +44-1223-336362
E-mail addresses: mjm14@cam.ac.uk (M.J. Mays), gas8@le.ac.uk (G.A. Solan).

0022-328X/02/$ - see front matter © 2002 Published by Elsevier Science B.V.
PII: S0022-328X(02)01892-2

2. Results and discussion

2.1. Reaction of [$Ru_3(CO)_{10}L_2$] (L = NCMe, CO) with *cyclo*-(PhX)$_6$ (X = As **1a**, P **1b**)

The reaction of [$Ru_3(CO)_{10}(NCMe)_2$] with an equimolar amount of *cyclo*-(PhX)$_6$ (X = As **1a**, P **1b**) in toluene at ambient temperature affords [$Ru_3\{\mu$-*cyclo*-(PhX)$_6\}(CO)_{10}$] (X = As **2a**, P **2b**) in high yield (Scheme 1). Both complexes have been characterised by IR, ^{1}H-, ^{31}P- (for **2b**), ^{13}C-NMR spectroscopy, mass spectrometry and by elemental analysis (see Table 1). In addition, the molecular structure for **2a** has been determined by single crystal X-ray diffraction. The molecular structure of **2a** is shown in Fig. 1 while selected bond distances and angles are listed in Table 2.

Crystals suitable for the analysis were grown by slow diffusion of hexane into a dichloromethane solution of **2a** at 0 °C. The structure of **2a** consists of a triangular Ru_3 core in which one edge is bridged by the two arsenic atoms in the 1,5 positions of the intact *cyclo*-hexaarsane ring. The average As–As–As angle of 93.5° in the arsenic ring is close to that in *cyclo*-(PhAs)$_6$ (91.0°) [9]. The As(1)–As(3)–As(2) angle of 89.3(1)°, is within the range of the values for the free ligand although noticeably larger than the corresponding angles in [$Co_2(\mu$-RCCR)$\{\mu$-*cyclo*-(PhAs)$_6\}(CO)_4$] (R = H, Ph) [5] and [$Co_2Fe(\mu_3$-S)$\{\mu$-*cyclo*-(PhAs)$_6\}(CO)_7$] [8]. This can be attributed to the difference in the metal–metal distances of these complexes. The bridged Ru–Ru bond is longer than the unbridged Ru–Ru bonds [2.888(1) Å as compared to 2.844(1) and 2.866(1) Å]. This elongation has also been observed with a number of triruthenium complexes in which a metal–metal edge is bridged by a diarsine ligand [10]. The ruthenium to arsenic average bond length of 2.485 Å for **2a** agree closely with the Ru–As distances in related species [10,11].

The spectroscopic properties of **2a** are in accord with the solid state structure being maintained in solution. The IR spectrum of **2a** exhibits three strong bands together with several weak bands in the terminal carbonyl region. The pattern of bands is very similar to those observed for other bis-equatorially substituted triruthenium and triosmium clusters [3a–3d]. On the basis of the close similarity of the IR data, complex **2b** is assigned a similar structure with phosphorus atoms in place of arsenic atoms. The FAB mass spectra for **2a** and **2b** both show molecular ion peaks and fragmentation peaks corresponding to the loss of up to 10 carbonyl groups. The one dimensional ^{31}P{^{1}H}-NMR spectrum of **2b** shows four multiplets at δ 39.2, 2.2, −5.8, −37.8, with an integral ratio of 1:2:2:1, respectively and consistent with **2b** possessing an approximate mirror plane of symmetry passing through the midpoint of the bridged Ru–Ru bond, P^2 and P^5 (see Scheme 1). On the basis of a two-dimensional COSY-90 ^{31}P-NMR spectroscopy, the four signals have been ascribed to P^2 (δ 39.2), P^1/P^3 (δ 2.2), P^4/P^6 (δ −5.8) and P^5 (δ −37.8).

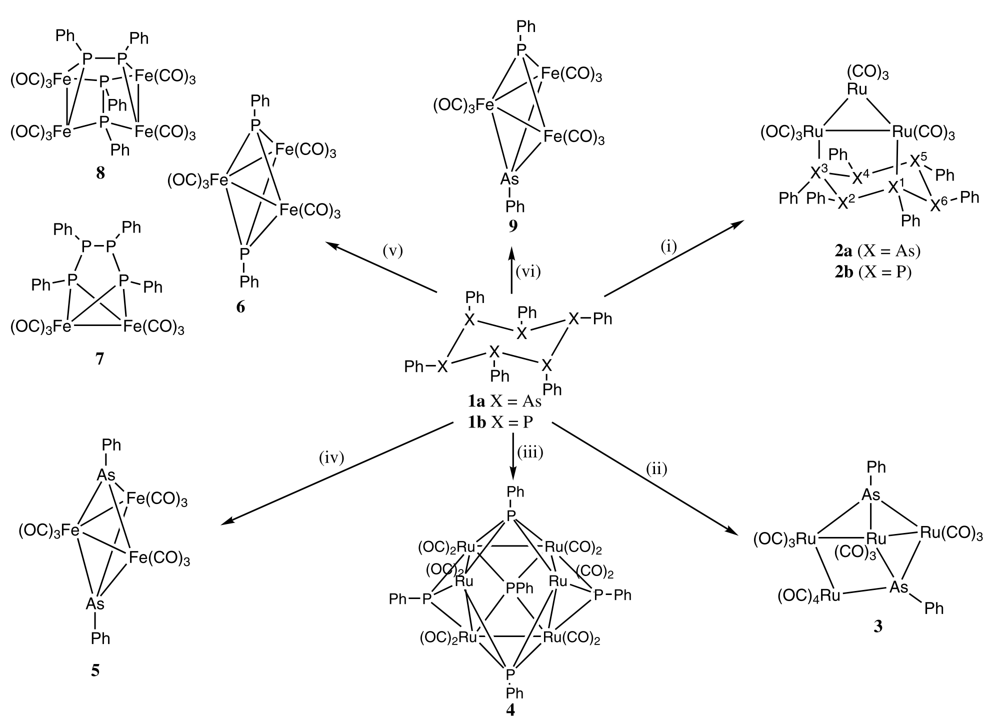

Scheme 1. *Reagents and conditions:* (i) [$Ru_3(CO)_{10}(NCMe)_2$], (**1a** or **1b**), room temperature; (ii) [$Ru_3(CO)_{12}$], (**1a**), toluene, heat; (iii) [$Ru_3(CO)_{12}$], (**1b**), heptane, heat; (iv) [$Fe_3(CO)_{12}$], toluene, heat, (**1a**); (v) [$Fe_3(CO)_{12}$], (**1b**), toluene, heat; (vi) [$Fe_3(CO)_{12}$], (**1a** and **1b**), toluene, heat.

Table 1
Spectroscopic and analytical data for the new complexes **2a**, **2b**, **3**, **5**, **8** and **9**

Compound	ν(CO) (cm^{-1}) [a]	^{1}H-NMR (δ) [b]	^{13}C-NMR (δ) [c]	^{31}P-NMR (δ) [d]	FAB mass spectrum	Microanalysis (%) [e]	
						C	H
2a	2086s, 2058w, 2028m, 2011vs, 1959m	8.1–6.4 [m, 30H, Ph]	211.0 [s, CO], 137–128 [m, Ph]		1495 ([$M^{+}-n$CO], $n=1$–10)	36.94 (36.89)	2.06 (2.02)
2b	2084s, 2025m, 2012vs, 1982m, 1958m	8.2–6.7 [m, 30H, Ph]	217.0 [m, CO], 137–127 [m, Ph]	39.2 [m, P(2)], 2.2 [m, P(1), P(3)], −5.8 [m, P(4), P(6)], −37.8 [m, P(5)]	1231 ([$M^{+}-n$CO], $n=1$–10)	44.50 (44.85)	2.47 (2.45)
3	2104m, 2070s, 2052vs, 2036s, 1995m	7.8–7.1 [m, 10H, Ph]	203.0 [s, 1CO], 199.6 [s, 1CO], 199.3 [br, 3CO], 198.0 [s, 1CO], 196.0 [s, 1CO], 194.0 [s, 3CO], 192.0 [s, 1CO], 191.0 [s, 1CO], 185.0 [s, 1CO], 147.0 [As*C*(Ph)], 144.0 [s, As*C*(Ph)], 132–128 [m, Ph]		1072 ([$M^{+}-n$CO], $n=1$–11)	28.08 (28.00)	0.95 (0.93)
5	2038vs, 2015s, 1996s	7.6 [m, 5H, Ph], 7.5 [m, 5H, Ph]	214.0 [s, CO], 207.0 [br, CO], 136–129 [m, Ph]		724 ([$M^{+}-n$CO], $n=1$–9)	35.56 (34.85)	1.60 (1.39)
8	2046vs, 2023s, 1998s, 1968m	7.4–6.9 [m, 20H, Ph]	213.0 [m, CO], 209.0 [m, CO], 208.0 [m, CO], 207.0 [m, CO], 135–127 [m, Ph]	536.0 [t, ^{2}J(PP) 174, 2P, (*P*Ph)$_2$], 233.0 [t, 2P, (*P*Ph)$_2$]	991 ([$M^{+}-n$CO], $n=1$–12)	43.37 (43.59)	2.07 (2.03)
9	2038vs, 2015s, 1997m	7.5–7.5 [m, Ph]	214.0 [m, CO], 213.6 [s, CO], 213.2 [s, CO], 212.3 [s, br, CO], 207.8 [br, CO], 138–128 [m, Ph]	339.0 [s, 1P, (PPh)]	680 ([$M^{+}-n$CO], $n=1$–9)	–	–

[a] Recorded in dichloromethane solution.
[b] ^{1}H-NMR chemical shifts (δ) in ppm relative to $SiMe_4$ (0.0 ppm), coupling constants in Hz in $CDCl_3$ at 293 K.
[c] Chemical shifts in ppm relative to $SiMe_4$ (0.0), in $CDCl_3$ at 293 K.
[d] ^{31}P-NMR chemical shifts (δ) in ppm relative to external 85% H_3PO_4 (0.0 ppm), {^{1}H}-gated decoupled, measured in $CDCl_3$ at 293 K.
[e] Calculated values in parentheses.

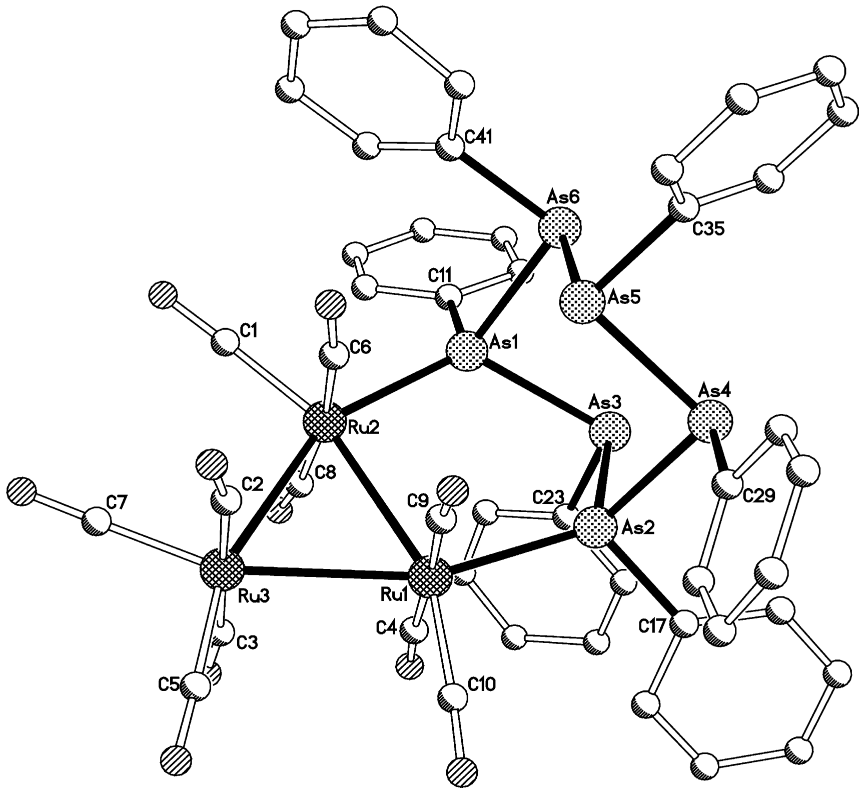

Fig. 1. Molecular structure of $[Ru_3\{\mu\text{-}cyclo\text{-}(PhAs)_6\}(CO)_{10}]$ (**2a**) including the atom numbering scheme. All hydrogen atoms have been omitted for clarity.

Table 2
Selected bond distances (Å) and angles (°) for **2a**

Bond distances			
Ru(1)–Ru(2)	2.888(1)	As(1)–As(6)	2.487(2)
Ru(2)–Ru(3)	2.866(1)	As(2)–As(3)	2.484(2)
Ru(1)–Ru(3)	2.844(1)	As(2)–As(4)	2.456(2)
Ru(1)–As(2)	2.474(1)	As(4)–As(5)	2.475(2)
Ru(2)–As(1)	2.496(1)	As(5)–As(6)	2.487(2)
As(1)–As(3)	2.477(2)	*Mean* Ru–C(carbonyl)	1.90
Bond angles			
Ru(1)–Ru(2)–Ru(3)	59.2(1)	As(2)–As(4)–As(5)	100.3(1)
Ru(1)–Ru(3)–Ru(2)	60.8(1)	As(3)–As(2)–As(4)	89.2(1)
Ru(2)–Ru(1)–Ru(3)	60.0(1)	As(3)–As(1)–As(6)	90.4(1)
As(1)–As(3)–As(2)	89.3(1)	As(4)–As(5)–As(6)	100.3(1)
As(1)–As(6)–As(5)	95.8(1)		

While conservation of the six-membered rings occurs on reaction of $[Ru_3(CO)_{10}(MeCN)_2]$ with **1a** and **1b**, fragmentation occurs when **1a** and **1b** are treated with one equivalent of $[Ru_3(CO)_{12}]$ at elevated temperatures. In the case of **1a** this leads to $[Ru_4(\mu_3\text{-}AsPh)_2(CO)_{13}]$ (**3**) and for **1b** to $[Ru_6(\mu_4\text{-}PPh)_3(\mu_3\text{-}PPh)_2(CO)_{12}]$ (**4**). Both **3** and **4** have been characterised by IR, ^{1}H-, ^{31}P- (for **4**), ^{13}C-NMR spectroscopy, mass spectrometry and by elemental analysis (see Table 1). In addition the molecular structures for **3** and **4** have been determined by single crystal X-ray diffraction. The molecular structure of **3** is shown in Fig. 2 while selected bond distances and angles are listed in Table 3. Crystals suitable for the analysis were grown by slow diffusion of

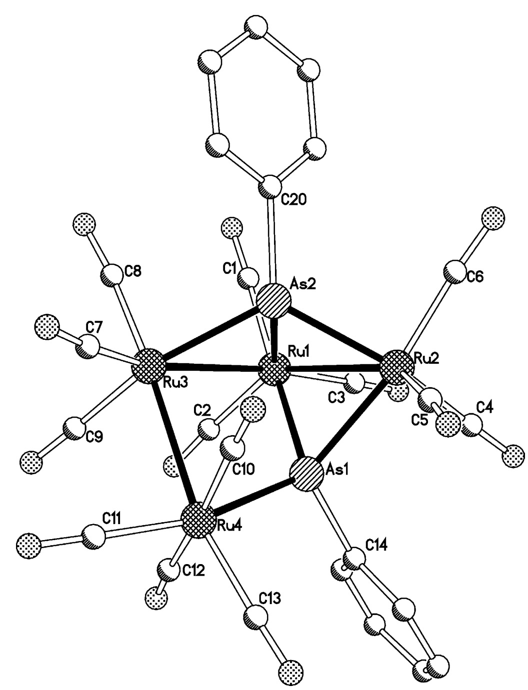

Fig. 2. Molecular structure of $[Ru_4(\mu_3\text{-}AsPh)_2(CO)_{13}]$ (**3**) including the atom numbering scheme. All hydrogen atoms have been omitted for clarity.

Table 3
Selected bond distances (Å) and angles (°) for **3**

Bond distances			
Ru(1)–Ru(2)	2.930(1)	Ru(2)–As(1)	2.461(1)
Ru(1)–Ru(3)	2.970(1)	Ru(2)–As(2)	2.434(1)
Ru(3)–Ru(4)	2.921(1)	Ru(3)–As(2)	2.448(1)
Ru(1)–As(1)	2.456(1)	Ru(4)–As(1)	2.496(1)
Ru(1)–As(2)	2.499(1)	*Mean* Ru–C(carbonyl)	1.91
Bond angles			
Ru(1)–As(1)–Ru(2)	73.2(1)	Ru(1)–As(2)–Ru(3)	73.8(1)
Ru(1)–As(1)–Ru(4)	114.9(1)	Ru(2)–As(2)–Ru(3)	124.2(1)
Ru(2)–As(1)–Ru(4)	124.2(1)	As(1)–Ru(1)–As(2)	77.8(1)
Ru(1)–As(2)–Ru(2)	72.9(1)	As(1)–Ru(2)–As(2)	78.9(1)

hexane into a dichloromethane solution of **3** at room temperature. The molecule consists of an open chain of four ruthenium atoms with two triply-bridging AsPh groups. The atom As(1) bridges Ru(4), Ru(1) and Ru(2) while As(2) bridges Ru(3), Ru(1) and Ru(2). Therefore, the Ru(1)–Ru(2) bond is bridged by both the phenylarsenidine groups forming a Ru_2As_2 butterfly unit. Each ruthenium atom is coordinated by three terminal carbonyl groups except Ru(4) which has four terminal carbonyl groups. All the ruthenium atoms have approximately octahedral geometry except Ru(1) which is seven-coordinate. The average Ru–Ru bond length of 2.94 Å, is longer than in $[Ru_3(CO)_{12}]$ (2.853 Å) [12] but within the normal range for Ru–Ru bond lengths [13].

Complex **3** has previously been obtained as a product from the reaction of $[Ru_3(CO)_{12}]$ with $[Cr(AsPhH_2)(CO)_5]$ although no experimental nor spectroscopic details were reported [14]. The spectroscopic properties of **3** are in accord with the solid state structure being maintained in solution. The IR spectrum of **3** shows five bands in the ν(CO) region which are similar to the structurally related tetraosmium complex $[Os_4(\mu_3\text{-}PCF_3)_2(CO)_{13}]$ [3d]. The $^{13}C\{^1H\}$-NMR spectrum at room temperature shows seven sharp and two broad signals in the carbonyl region corresponding to the 13 carbonyl groups. This suggests that six carbonyl groups on two ruthenium atoms are fluxional at room temperature. By inspection of the crystal structure it was revealed that the rotation of the three carbonyl groups residing on Ru(3) is hindered by the four carbonyl groups on Ru(4). Therefore, the two broad signals can most likely be attributed to the rapid trigonal rotation of the three carbonyl ligands on each of the Ru(1) and Ru(2) atoms.

The molecular structure of $\mathbf{4}\cdot 2CH_2Cl_2$ is shown in Fig. 3 while selected bond distances and angles are listed in Table 4. Crystals suitable for the analysis were grown by diffusion of hexane into a dichloromethane solution of **4** at 0 °C. A different crystallographic modification of **4**, in which no solvate is present, has been reported previously [15]. The structure of $\mathbf{4}\cdot 2CH_2Cl_2$ is essentially the same as the non-solvated form with the six ruthenium atoms [Ru(1), Ru(2), Ru(3), Ru(1A), Ru(2A), Ru(3A)], adopting a distorted trigonal prismatic geometry with all the triangular and square faces capped by phenylphosphinidene ligands and each ruthenium atom bound by two carbonyl ligands. The principal difference between $\mathbf{4}\cdot 2CH_2Cl_2$ and **4** [15] is

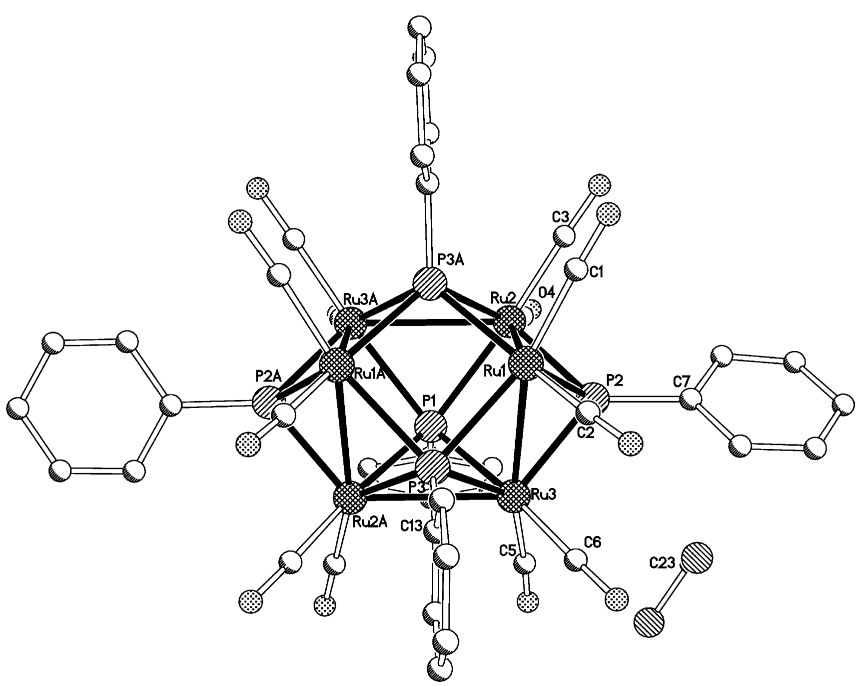

Fig. 3. Molecular structure of $[Ru_6(\mu_4\text{-}PPh)_3(\mu_3\text{-}PPh)_2(CO)_{12}]$ ($\mathbf{4}\cdot 2CH_2Cl_2$) including the atom numbering scheme. All hydrogen atoms have been omitted for clarity.

Table 4
Selected bond distances (Å) and angles (°) for $4\cdot 2CH_2Cl_2$

Bond distances			
Ru(1)–Ru(2)	2.895(1)	Ru(2)–P(1)	2.481(2)
Ru(1)–Ru(3)	2.900(1)	Ru(2)–P(3A)	2.358(3)
Ru(1)···Ru(1A)	3.265(1)	Ru(2)–P(2)	2.277(3)
Ru(2)–Ru(3A)	2.937(1)	Ru(3)–P(1)	2.474(2)
Ru(2A)–Ru(3)	2.937(1)	Ru(3)–P(2)	2.288(3)
Ru(2)···Ru(3)	3.417(2)	Ru(3)–P(3)	2.352(3)
Ru(1)–P(3)	2.431(3)	*Mean* Ru–C(carbonyl)	1.90
Ru(1)–P(2)	2.306(3)		
Bond angles			
Ru(1)–Ru(2)–Ru(3)	53.9(1)	Ru(2)–P(1)–Ru(3)	72.7(1)
Ru(1)–Ru(2)–Ru(3A)	93.3(1)	Ru(2)–Ru(1)–Ru(3)	72.3(1)
Ru(1)–Ru(3)–Ru(2)	53.8(1)	Ru(2)–Ru(1)–Ru(1A)	86.8(1)
Ru(1)–Ru(3)–Ru(2A)	93.3(1)	Ru(2)–Ru(3)–Ru(2A)	90.1(1)
Ru(1)–P(2)–Ru(3)	78.3(1)	Ru(2)–P(3A)–Ru(1)	74.3(1)
Ru(1)–P(3)–Ru(3)	74.6(1)	Ru(3)–P(3)–Ru(2A)	77.1(1)
Ru(1)–P(2)–Ru(2)	78.4(1)		

that in the solvate form the molecule lies on a crystallographically twofold axis passing through P(1), C(19) and C(22). This has the effect that in $\mathbf{4}\cdot 2CH_2Cl_2$ the distortion or expansion of the metal atom framework from a regular trigonal prismatic geometry occurs symmetrically about the twofold axis through P(1) [Ru(2)–Ru(3) 3.417(2) and Ru(3A)–Ru(2A) 3.417(2) Å]. On the other hand, in **4** [15] the expansion occurs unsymmetrically with the elongation of the corresponding ruthenium–ruthenium edges differing by 0.186 Å. In addition, the Ru(1)···Ru(1A) non-bonded distance [3.265(1) Å] in $\mathbf{4}\cdot 2CH_2Cl_2$, which corresponds to an axial edge of the trigonal prism, is marginally longer than in the non-solvated form [3.323(3) Å].

The spectroscopic properties of **4** are consistent with those previously reported. It is noteworthy that the yield of 25% for **4** obtained using the methodology described in this paper is an improvement on that previously reported (15%), in which **4** was prepared from the reaction of $[Ru_3(CO)_{12}]$ with three equivalents of phenylphosphine [15].

2.2. Reaction of $[Fe_3(CO)_{12}]$ with *cyclo*-$(PhX)_6$ (X = As **1a**, P **1b**)

The reaction of **1a** with two equivalents of $Fe_3(CO)_{12}$ in toluene at elevated temperature gives $[Fe_3(\mu_3\text{-AsPh})_2(CO)_9]$ (**5**) in good yield. The corresponding reaction of **1b** affords the complexes $[Fe_3(\mu_3\text{-PPh})_2(CO)_9]$ (**6**), $[Fe_2(\mu\text{-}\eta^2\text{-}catena\text{-}(P_4Ph_4))(CO)_6]$ (**7**) and $[Fe_2\{\mu_4\text{-}(P_2Ph_2)\}(CO)_6]_2$ (**8**) in overall moderate yield (Scheme 1). All the complexes have been characterised by IR, ^{1}H-, ^{31}P- (**6**–**8**), ^{13}C-NMR spectroscopy, mass spectrometry and by elemental analysis (see Table 1).

The isostructural trigonal bipyramidal complexes **5** and **6** have been previously synthesised by alternative routes and crystallographically characterised [16–18]. Evans and coworkers reported the synthesis of **6** from the reaction of $[Fe_3(CO)_{12}]$ with phenylphosphine [16] and thus **6** has been identified on the basis of the close similarity of the spectroscopic data. However, in the case of **5** no previous spectroscopic data were available due to the low yields of the reaction methods employed [17,18].

In the IR spectrum of **5**, three strong bands are seen in the terminal carbonyl region due to the presence of the nine carbonyl groups in a pattern that is closely related to that for **6**. The $^{13}C\{^{1}H\}$-NMR spectrum of **5** displays a sharp peak at δ 214.0 and a broad peak at δ 207.0 for the nine terminal carbonyl ligands in addition to the phenyl resonances. A similar pair of signals in the carbonyl region has also been observed for **6**, in which the sharp signal has been assigned to a rotating central $Fe(CO)_3$ group and the broader resonance to intermediate exchange behaviour involving more restricted localised rotation of the two outer $Fe(CO)_3$ units [16]. It is likely that a similar mechanism is also operating for **5**. The FAB mass spectrum of **5** shows a molecular ion peak along with fragmentation peaks corresponding to the loss of up to nine carbonyl groups.

Complex **7** has been characterised on the basis of the close similarity of the spectroscopic properties with those previously reported [19]. In addition, the unit cell dimensions of a single crystal obtained in this work are closely related to the crystallographically determined structure of **7** [20]. Notably, West and Ang prepared **7** as the sole product from the reaction of $[Fe(CO)_5]$ with either *cyclo*-$(PhP)_4$ or *cyclo*-$(PhP)_5$ in a sealed tube at elevated temperature. However, employment of the larger CPP, **1b**, under similar conditions has furnished **7** along with two other complexes (**6** and **8**), all resulting from fragmentation of the CPP ring.

The molecular structure of **8** is shown in Fig. 4 while selected bond distances and angles are collected in Table

Table 5
Selected bond distances (Å) and angles (°) for **8**

Bond distances			
Fe(1)–Fe(2)	2.732(2)	Fe(3)–P(2)	2.210(3)
Fe(3)–Fe(4)	2.738(2)	Fe(4)–P(2)	2.205(2)
P(1)–P(2)	2.232(3)	Fe(1)–P(4)	2.347(3)
P(3)–P(4)	2.205(3)	Fe(3)–P(4)	2.313(3)
Fe(1)–P(1)	2.206(3)	Fe(2)–P(3)	2.319(3)
Fe(2)–P(1)	2.200(3)	Fe(4)–P(3)	2.352(3)
Mean Fe–C(carbonyl)	1.78		
Bond angles			
Fe(1)–P(1)–Fe(2)	76.7(1)	Fe(3)–P(4)–P(3)	95.5(1)
Fe(1)–P(4)–Fe(3)	119.2(1)	Fe(3)–Fe(4)–P(3)	81.8(1)
Fe(1)–Fe(2)–P(3)	84.9(1)	Fe(4)–P(3)–P(4)	97.5(1)
Fe(1)–P(4)–P(3)	97.5(1)	Fe(4)–Fe(3)–P(4)	85.0(1)
Fe(2)–P(3)–Fe(4)	119.6(1)	P(1)–P(2)–Fe(4)	111.0(1)
Fe(2)–P(3)–P(4)	95.3(1)	P(1)–P(2)–Fe(3)	117.1(1)
Fe(2)–Fe(1)–P(4)	82.0(1)		

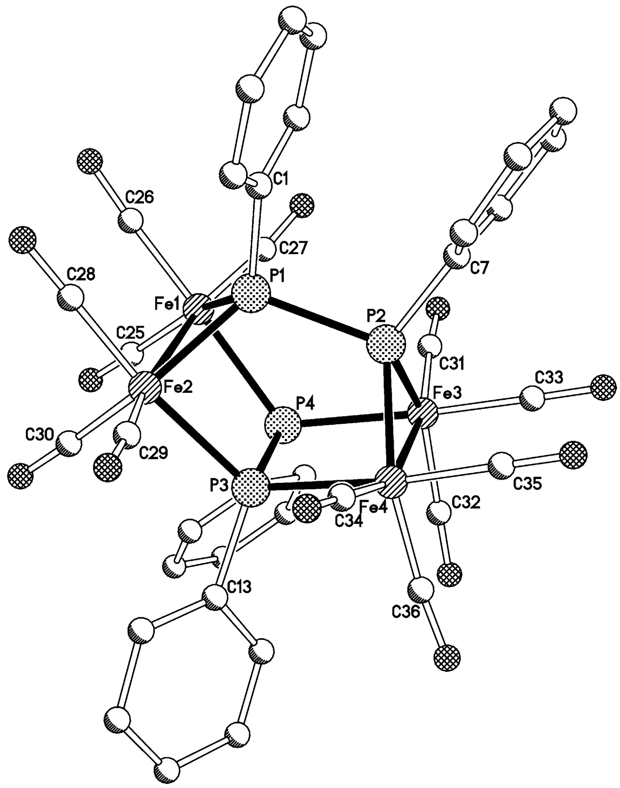

Fig. 4. Molecular structure of $[Fe_2\{\mu_4\text{-}(P_2Ph_2)\}(CO)_6]_2$ (**8**) including the atom numbering scheme. All hydrogen atoms have been omitted for clarity.

5. Crystals suitable for the analysis were grown by diffusion of hexane into a dichloromethane solution of **8** at 0 °C. The molecule is constructed from two discrete metal–metal bonded $Fe_2(CO)_6$ units linked together by two diphenyldiphosphane groups. One of the P_2Ph_2 moieties bridges the Fe–Fe vectors perpendicularly with each phosphorus atom [P(1), P(2)] bonded to both iron atoms of a particular $Fe_2(CO)_6$ unit. The other P_2Ph_2 moiety bridges the Fe–Fe vectors in a parallel bonding mode with each phosphorus atom [P(3), P(4)] linked to metal atoms belonging to different $Fe_2(CO)_6$ units. The Fe–Fe iron bond lengths [2.732(2), 2.738(2) Å] fall into the typical range for complexes of a similar type and the average Fe–P bond length of 2.27 Å, is in the range observed for other bridging diphosphane and phosphido groups bound to an iron carbonyl moiety [21]. The P–P bond lengths of 2.232(3) and 2.205(3) Å are consistent with single bonds between the two atoms.

Complex **8** can be considered as belonging to a family of compounds of general formula $[(OC)_3FePR]_4$. Indeed Vahrenkamp and coworker have structurally characterised the complex $[(OC)_3FePMe]_4$, which can be viewed as a structural isomer of **8**, in which both diphosphane ligands perpendicularly bridge both $Fe_2(CO)_6$ units [21c]. Indeed Vahrenkamp has previously suggested that a complex of type **8** should be obtainable and has related its structure to the hydrocarbon cuneane [22].

The IR spectrum of **8** exhibits three strong bands and one medium intensity band in the terminal ν(CO) region due to the presence of the 12 carbonyl groups. These values are consistent with the pattern of bands observed for the related complex $[(OC)_3FePMe]_4$ [21c]. The $^{13}C\{^1H\}$-NMR spectrum at room temperature shows, in addition to signals for the four phenyl groups, four broad resonances at δ 213.0, 211.0, 209.0 and 207.0 due to the terminal carbonyl groups. It would seem likely that at this temperature a fluxional process is operating. In the $^{31}P\{^1H\}$-NMR spectrum of **8**, two triplets at δ 536.0 and 233.0 [^2J(PP) 174 Hz] correspond to the four phosphorus atoms of the two P_2Ph_2 groups suggesting that two phosphorus atoms on a given P_2Ph_2 ligand are equivalent to each other. The FAB mass spectrum of **5** shows a molecular ion peak along with fragmentation peaks corresponding to the loss of up to 12 carbonyl groups.

Given the propensity of **1a** or **1b** to act as sources of AsPh and PPh fragments when reacted with $[Fe_3(CO)_{12}]$, we decided to attempt a preparation of an iron complex containing both AsPh and PPh ligands. The reaction of $[Fe_3(CO)_{12}]$ with **1a** and **1b** in a 2:1:1 molar ratio at elevated temperature gave **5**, **6** and $[Fe_3(\mu_3\text{-PPh})(\mu_3\text{-AsPh})(CO)_9]$ (**9**) in moderate overall yield (Scheme 1). All three complexes have the same retention factor (R_f) and could not be separated by chromatographic means. However, the presence of the three complexes could be identified from the spectroscopic data and by comparing these data with those for the already characterised complexes **5** and **6**. For example, in the $^{31}P\{^1H\}$-NMR spectrum of the mixture, an additional peak for the PPh ligand in **9** is seen at δ 339.4. The FAB mass spectrum displays molecular ion peaks for **5** and **6** along with that for **9** in addition to fragmentation peaks corresponding to carbonyl losses for each complex.

3. Summary

The reactions of the hexaphenyl *cyclo*-hexaarsane **1a** and *cyclo*-hexaphosphane **1b** with a ruthenium cluster containing labile ligands, $[Ru_3(CO)_{10}(NCMe)_2]$, lead to the products **2a** and **2b** in which the six-membered rings of the ligands remain intact. However, notable differences are observed in the outcome of the reactions of **1a** and **1b** with metal clusters containing only carbonyl ligands. Thus, the reactions of **1a** with $[Ru_3(CO)_{12}]$ and $[Fe_3(CO)_{12}]$ yield the complexes **3** and **5**, respectively, containing triply-bridging phenylarsenidene units as the sole Group 15 ligand, indicating extensive disruption of the hexameric arsenic ring. In contrast, the reactions of **1b** with $[Ru_3(CO)_{12}]$ and $[Fe_3(CO)_{12}]$ under similar conditions yield **4**, **6**, **7** and **8**, in which varying degrees of fragmentation of the cyclic phosphorus rings occur. Finally, a mixed arsenidene–phosphinidene iron complex **9** has been shown to be accessible.

4. Experimental

4.1. General techniques

All reactions were carried out under an atmosphere of dry, oxygen-free nitrogen, using standard Schlenk techniques. Solvents were distilled under nitrogen from appropriate drying agents and degassed prior to use [23]. IR spectra were recorded in C_6H_{14} solution in 0.5 mm NaCl cells, using a Perkin–Elmer 1710 Fourier-transform spectrometer. Fast atom bombardment (FAB) mass spectra were recorded on a Kratos MS 890 instrument using 3-nitrobenzyl alcohol as a matrix. Proton (reference to $SiMe_4$), ^{31}P- and ^{13}C-NMR spectra were recorded on either a Bruker WM250 or AM400 spectrometer, ^{31}P-NMR chemical shifts are referenced to 85% H_3PO_4. Preparative thin-layer chromatography (TLC) was carried out on commercial Merck plates with a 0.25 mm layer of silica, or on 1 mm silica plates prepared at the Department of Chemistry, Cambridge. Column chromatography was performed on Kieselgel 60 (70–230 or 230–400 mesh). Products are given in order of decreasing R_f values. Elemental analyses were performed at the Department of Chemistry, Cambridge.

Unless otherwise stated all reagents were obtained from commercial suppliers and used without further purification. The syntheses of $[Ru_3(CO)_{10}(NCMe)_2]$ [24], **1a** [25] and **1b** [26] have been reported previously.

4.2. Synthesis of **2**

4.2.1. Complex **2a**

To a solution of $[Ru_3(CO)_{10}(NCMe)_2]$ (0.131 g, 0.2 mmol) in $C_6H_5CH_3$ (50 ml) was added **1a** (0.183 g, 0.20 mmol) and the resulting solution stirred at ambient temperature for 6 h. After removal of solvent at reduced pressure, the residue was dissolved in the minimum volume of CH_2Cl_2 and applied to the base of preparative TLC plates. Elution using C_6H_{14}–CH_2Cl_2 (4:1) gave reddish–orange crystalline $[Ru_3\{\mu\text{-}cyclo\text{-}(PhAs)_6\}(CO)_{10}]$ (**2a**) (0.20 g, 67%).

4.2.2. Complex **2b**

To a solution of $[Ru_3(CO)_{10}(NCMe)_2]$ (0.061 g, 0.09 mmol) in C_6H_6 (50 ml) was added **1b** (0.065 g, 0.10 mmol) and the resulting solution stirred at ambient temperature overnight. After removal of the solvent under reduced pressure, the residue was dissolved in the minimum volume of CH_2Cl_2 and purified by preparative TLC. Elution using C_6H_{14}–CH_2Cl_2 (4:1) gave dark orange crystalline $[Ru_3\{\mu\text{-}cyclo\text{-}(PhP)_6\}(CO)_{10}]$ (**2b**) (0.07 g, 63%).

4.3. Synthesis of **3**

The complex $[Ru_3(CO)_{12}]$ (0.159 g, 0.25 mmol) and **1a** (0.23 g, 0.25 mmol) were dissolved in $C_6H_5CH_3$ (10 ml) and the reaction vessel evacuated with three freeze–pump–thaw cycles then sealed under reduced pressure. The reaction mixture was stirred at 70 °C for 24 h. After cooling the reaction vessel was opened and the solution filtered. Following removal of the solvent under reduced pressure, the residue was redissolved in CH_2Cl_2, silica added and the mixture pumped dry. The solid was added to the top of a silica chromatography column; elution with C_6H_{14} gave unreacted $[Ru_3(CO)_{12}]$ and the dark yellow crystalline compound $[Ru_4(\mu_3\text{-}PhAs)_2(CO)_{13}]$ (**3**) (0.025 g, 9%).

4.4. Synthesis of **4**

To a solution of $[Ru_3(CO)_{12}]$ (0.20 g, 0.31 mmol) in C_7H_{16} (50 ml) was added **1b** (0.20 g, 0.30 mmol) and the resulting solution heated to reflux for 5 h. The solution was then cooled to room temperature (r.t.) and filtered. After removal of the solvent under reduced pressure, the residue was dissolved in the minimum volume of CH_2Cl_2 and applied to the base of TLC plates. Elution with C_6H_{14}–CH_2Cl_2 (4:1) gave unreacted starting material, green $[Ru_6(\mu_4\text{-}PPh)_3(\mu_3\text{-}PPh)_2(CO)_{12}]$ (**4**) (0.005 g, 12%) and trace quantities of uncharacterised red and brown compounds.

4.5. Synthesis of **5**

To a solution of **1a** (0.456 g, 0.5 mmol) in $C_6H_5CH_3$ (50 ml) was added $[Fe_3(CO)_{12}]$ (0.510 g, 1.0 mmol). The solution was heated to 90 °C for 5 h. The solution was then cooled to r.t. and filtered. After removal of the solvent under reduced pressure, the residue was redissolved in CH_2Cl_2, silica added and the mixture pumped dry. The solid was added to the top of a silica chromatography column and elution with C_6H_{14}–CH_2Cl_2 (4:1) gave $[Fe_3(\mu_3\text{-}AsPh)_2(CO)_9]$ (**5**) (0.219 g, 65%).

4.6. Synthesis of **6**, **7** and **8**

$[Fe_3(CO)_{12}]$ (0.504 g, 1.0 mmol) and **1b** (0.324 g, 0.50 mmol) were dissolved in $C_6H_5CH_3$ (10 ml); the reaction vessel was then evacuated with three freeze–pump–thaw cycles and sealed under reduced pressure. The mixture was stirred at 90 °C for 24 h and, after cooling, the vessel was then opened and the solution filtered. After removal of the solvent under reduced pressure, the residue was dissolved in the minimum volume of

Table 6
Crystallographic and data processing parameters for complexes **2a**, **3**, **4**·$2CH_2Cl_2$ and **8**

Complex	**2a**	**3**	**4**	**8**
Empirical formula	$C_{46}H_{30}As_6O_{10}Ru_3$	$C_{25}H_{10}As_2O_{13}Ru_4$	$C_{42}H_{26}O_{12}P_5Ru_6\cdot$**2**$CH_2Cl_2$	$C_{36}H_{20}Fe_4O_{12}P_4$
M	1495.43	1072.45	1653.75	991.80
Temperature (K)	293(2)	150(2)	150(2)	180(2)
Crystal system	Monoclinic	Monoclinic	Monoclinic	Monoclinic
Space group	$P2_1/n$	$P2_1/c$	$C2/c$	$P2_1/n$
Lattice parameters				
a (Å)	13.043(5)	11.430(4)	13.030(3)	10.7290(10)
b (Å)	22.614(5)	16.968(3)	27.338(3)	16.1130(10)
c (Å)	17.244(5)	16.110(3)	16.832(40)	24.1250(10)
α (°)	90	90	90	90
β (°)	100.44(3)	92.02(2)	107.45(2)	96.380(10)
γ (°)	90	90	90	90
U (Å^3)	5002	3122.5(14)	5720(2)	4144.8(5)
Z	4	4	4	4
D_{calc} (mg m^{-3})	1.986	2.281	1.920	1.589
μ(Mo–K$_\alpha$) (mm^{-1})	4.877	4.063	1.924	1.584
F(000)	2864	2024	3188	1984
Crystal size (mm)	0.15 × 0.10 × 0.05	0.20 × 0.18 × 0.10	0.20 × 0.10 × 0.10	0.20 × 0.10 × 0.10
Reflections collected	6530	5782	6853	18 963
Independent reflections	6208	5489	6571	6636
R_{int}	0.037	0.044	0.085	0.088
Parameters/restraints	586/0	397/0	306/3	505/0
Final R indices [$I > 2\sigma(I)$]	$R_1 = 0.0501$, $wR_2 = 0.1172$	$R_1 = 0.0458$, $wR_2 = 0.0940$	$R_1 = 0.0597$, $wR_2 = 0.1306$	$R_1 = 0.0558$, $wR_2 = 0.1385$
All data	$R_1 = 0.0712$, $wR_2 = 0.1302$	$R_1 = 0.0743$, $wR_2 = 0.1063$	$R_1 = 0.1778$, $wR_2 = 0.2184$	$R_1 = 0.1434$, $wR_2 = 0.1651$
Goodness-of-fit on F^2 (all data)	1.045	1.048	1.006	0.996

Data in common: graphite-monochromated Mo–K$_\alpha$ radiation, $\lambda = 0.71073$ Å; $R_1 = \Sigma\,||F_o|-|F_c||/\Sigma\,|F_o|$, $wR_2 = [\Sigma\,w(F_o^2-F_c^2)^2/\Sigma\,w(F_o^2)^2]^{1/2}$, $w^{-1} = [\sigma^2(F_o)^2+(aP)^2]$, $P = [\max(F_o^2,\ 0)+2(F_c^2)]/3$, where a is a constant adjusted by the program; goodness-of-fit $= [\Sigma\,(F_o^2-F_c^2)^2/(n-p)]^{1/2}$ where n is the number of reflections and p the number of parameters.

CH_2Cl_2 and separated by preparative TLC. Elution using C_6H_{14}–CH_2Cl_2 (4:1) gave orange crystalline [$Fe_3(\mu_3\text{-}PPh_2)_2(CO)_9$] (**6**) (0.04 g, 15%), yellow crystalline [$Fe_2\{\mu\text{-}\eta^2\text{-}catena\text{-}(P_4Ph_4)\}(CO)_6$] (**7**) (0.02 g, 7%) and orange crystalline [$Fe_2\{\mu_4\text{-}(P_2Ph_2)\}(CO)_6]_2$ (**8**) (0.02 g, 5%).

4.7. Synthesis of 9

[$Fe_3(CO)_{12}$] (0.504 g, 1.0 mmol), **1b** (0.324 g, 0.50 mmol) and **1a** (0.324 g, 0.50 mmol) were dissolved in $C_6H_5CH_3$ (15 ml); the reaction vessel was then evacuated with three freeze–pump–thaw cycles and sealed under reduced pressure. The mixture was stirred at 90 °C for 24 h; after cooling the vessel was then opened and the solution filtered. After removal of the solvent under reduced pressure, the residue was dissolved in the minimum volume of CH_2Cl_2 and separated by preparative TLC. Elution using C_6H_{14}–CH_2Cl_2 (4:1) gave a mixture of [$Fe_3(\mu_3\text{-}AsPh)_2(CO)_9$] (**5**), [$Fe_3(\mu_3\text{-}PPh_2)_2(CO)_9$] (**6**) and [$Fe_3(\mu_3\text{-}AsPh_2)(\mu_3\text{-}PPh_2)(CO)_9$] (**9**) as a red–orange solid (0.133 g).

4.8. Crystallography

X-ray intensity data was collected using Rigaku AFC7R (**2a**, **3**, **4**) and RAXIS-IIC image plate diffractometers (**8**). Both systems were equipped with an Oxford Cryosystems Cryostream. Details of data collection, refinement and crystal data are listed in Table 6. Semiempirical absorption corrections based on φ-scan data were applied [27,28] to the data for **2a**, **3**, **4** and **7**. No absorption correction was applied to the data for **8**. The structures were solved by direct methods (SHELXS-86 [29]) and subsequent Fourier-difference syntheses and refined anisotropically on all ordered non-hydrogen atoms by full-matrix least-squares on F^2 (SHELXL-93 [30]). Hydrogen atoms were placed in geometrically idealised positions and refined using a riding model. In the final cycles of refinement a weighting scheme was introduced which produced a flat analysis of variance.

5. Supplementary material

Crystallographic data for the structural analysis have been deposited with the Cambridge Crystallographic Data Centre, CCDC nos. 184273–184276 for compounds **2a**, **3**, **4**·$2CH_2Cl_2$ and **8**. Copies of this information may be obtained free of charge from The Director, CCDC, 12 Union Road, Cambridge CB2 1EZ, UK (Fax: +44-1223-336033; e-mail: deposit@ccdc.cam.ac.uk or www: http://www.ccdc.cam.ac.uk).

Acknowledgements

We gratefully acknowledge the financial support of the Cambridge Commonwealth Trust and the United Kingdom Committee of Vice Chancellors and Principals (to R.M.D.S.). Thanks is also due to Dr J.E. Davis for collection of the X-ray data.

References

[1] (a) A.-J. DiMaio, A.L. Rheingold, Chem. Rev. 90 (1990) 169;
(b) A.L. Rheingold, in: A.L. Rheingold (Ed.), Homoatomic Rings, Chains and Macromolecules of the Main-Group Elements, Elsevier, Amsterdam, 1977, p. 385.
[2] For reactions involving CPAs see for example: (a) A.L. Rheingold, M.E. Fountain, Organometallics 5 (1986) 2410;
(b) A.L. Rheingold, M.E. Fountain, A.J. DiMaio, J. Am. Chem. Soc. 109 (1987) 141;
(c) P.S. Elmes, B.O. West, Aust. J. Chem. 23 (1970) 2247;
(d) P.S. Elmes, B.M. Gatehouse, D.J. Lloyd, B.O. West, J. Chem. Soc. Chem. Commun. (1974) 953;
(e) P.S. Elmes, B.O. West, J. Organomet. Chem. 32 (1971) 365;
(f) P.S. Elmes, P. Laverett, B.O. West, J. Chem. Soc. Chem. Commun. (1971) 747;
(g) A.L. Rheingold, M.J. Foley, P.J. Sullivan, Organometallics 1 (1982) 1429;
(h) A.L. Rheingold, M.R. Churchill, J. Organomet. Chem. 243 (1983) 165;
(i) B.M. Gatehouse, J. Chem. Soc. Chem. Commun. (1969) 948;
(j) A.L. Rheingold, P.J. Sullivan, J. Chem. Soc. Chem. Commun. (1983) 39;
(k) A.L. Rheingold, P.J. Sullivan, Organometallics 1 (1982) 1547;
(l) L.F. Dahl, A.S. Foust, M.S. Foster, J. Am. Chem. Soc. 24 (1969) 5631.
[3] For reactions involving CPPs see for example: (a) H.-G. Ang, L.-L. Koh, Q. Zhang, J. Chem. Soc. Dalton Trans. (1995) 2757;
(b) H.-G. Ang, S.-G. Ang, Q. Zhang, J. Chem. Soc. Dalton Trans. (1996) 2773;
(c) H.-G. Ang, S.-G. Ang, Q. Zhang, J. Chem. Soc. Dalton Trans. (1996) 3843;
(d) H.-G. Ang, K.-W. Ang, S.-G. Ang, A.L. Rheingold, J. Chem. Soc. Dalton Trans. (1996) 3131;
(e) R.A. Bartlett, H.V.R. Dias, K.M. Flynn, H. Hope, B.D. Murray, M.M. Olmstead, P.P. Power, J. Am. Chem. Soc. 109 (1987) 5693;
(f) M. Bandler, F. Slazer, J. Hahn, E. Därr, Angew. Chem. Int. Ed. Engl. 24 (1985) 415;
(g) B.F.G. Johnson, T.M. Layer, J. Lewis, P.R. Raithby, W.-T. Wong, J. Chem. Soc. Dalton Trans. (1993) 973.
[4] Most previous studies (see Refs. [1–3]) of CPAs and CPPs have been performed using elevated temperatures and/or in sealed vessels.
[5] R.M. De Silva, M.J. Mays, J.E. Davies, P.R. Raithby, M.A. Rennie, G.P. Shield, J. Chem. Soc. Dalton Trans. (1998) 439.
[6] R.M. De Silva, M.J. Mays, G.A. Solan, unpublished results.
[7] R.M. De Silva, M.J. Mays, P.R. Raithby, G.A. Solan, J. Organomet. Chem. 625 (2001) 245.
[8] R.M. De Silva, M.J. Mays, P.R. Raithby, G.A. Solan, J. Organomet. Chem. 642 (2002) 237.
[9] (a) K. Hedberg, E.W. Hughes, J. Waser, Acta Crystallogr. 14 (1961) 369;
(b) A.L. Rheingold, P.J. Sullivan, Organometallics 2 (1983) 327.
[10] (a) S.G. Teoh, H.K. Fun, O.B. Shawkataly, Z. Kristallogr. 190 (1990) 287;
(b) P.J. Roberts, J. Trotter, J. Chem. Soc. Sect. A (1971) 1479;
(c) P.J. Roberts, J. Trotter, J. Chem. Soc. Sect. A (1970) 3246.
[11] (a) G. Lavigne, N. Lugan, J.-J. Bonnet, Organometallics 1 (1982) 1040;
(b) O.B. Shawkataly, K. Ramalingam, S.T. Lee, M. Parameswary, H.K. Fun, K. Sivakumar, Polyhedron 17 (1998) 1211.
[12] M.R. Churchill, F.J. Hollander, J.P. Hutchinson, Inorg. Chem. 16 (1977) 2655.
[13] The 'normal' range for Ru–Ru bonds are in the range 2.70–2.95 Å, see: H.-G. Ang, S.-G. Ang, S.-W. Du, B.-H. Sow, A.L. Rheingold, J. Organomet. Chem. 510 (1996) 13 (and references therein),
[14] J.S. Field, R.J. Haines, D.N. Smit, K. Natarajan, O. Scheidsteger, G. Huttner, J. Organomet. Chem. 2140 (1982) C23.
[15] J.S. Field, R.J. Haines, D.N. Smit, J. Chem. Soc. Dalton Trans. (1988) 1315.
[16] S.L. Cook, J. Evans, L.R. Gray, M. Webster, J. Organomet. Chem. 236 (1982) 367.
[17] G. Huttner, G. Mohr, A. Frank, U. Schubert, J. Organomet. Chem. 118 (1976) C73.
[18] M. Jacob, E. Weiss, J. Organomet. Chem. 131 (1977) 263.
[19] H.-G. Ang, B.O. West, Aust. J. Chem. 20 (1967) 1133.
[20] A.L. Rheingold, M.E. Fountain, Organometallics 3 (1984) 1417.
[21] See for example: (a) H. Vahrenkamp, D. Wolters, Angew Chem. Int. Ed. Engl. 22 (1983) 154;
(b) E.P. Kyba, K.L. Hassett, B. Sheikh, J.S. McKennis, R.B. King, R.E. Davis, Organometallics 4 (1985) 994;
(c) R.L. De, H. Vahrenkamp, Angew. Chem. Int. Ed. Engl. 23 (1984) 983;
(d) W. Clegg, Inorg. Chem. 15 (1976) 1609.
[22] L.R. Smith, J. Chem. Edu. 55 (1978) 569.
[23] W.L.F. Armarego, D.D. Perrin, Purification of Laboratory Chemicals, 4th ed., Butterworth, Heinemann, 1996.
[24] G.A. Foulds, B.F.G. Johnson, J. Lewis, J. Organomet. Chem. 296 (1985) 147.
[25] (a) K. Hedberg, E.W. Hughes, J. Waser, Acta Crystallogr. 14 (1961) 369;
(b) A.L. Rheingold, P.J. Sullivan, Organometallics 2 (1983) 327.
[26] (a) J.J. Daly, J. Chem. Soc. Sect. A (1966) 428;
(b) J.J. Daly, J. Chem. Soc. (1965) 4789.
[27] TEXSAN, Version 1.1-1, Molecular Structure Corporation, The Woodlands, TX, 1985, 1992, 1995.
[28] A.C.T. North, D.C. Philips, F.S. Mathews, Acta Crystallogr. Sect. A 24 (1968) 351.
[29] G.M. Sheldrick, SHELXS-86, University of Göttingen, 1993.
[30] G.M. Sheldrick, SHELXL-93, University of Göttingen, 1993.